A Novel Reduction Strategy of Standby Power Loss in the Multi-Oscillated Current Resonant DC-DC Converter Considering Acoustic Noise Compatibility

Tadahiko SATO [1, 2], Hirofumi MATSUO [2] and Hiroyuki OTA[1]

1) Fuji Electric Co., Ltd.
2) Graduate School of Science and Technology, Nagasaki University
E-mail: sato-tadahiko@fujielectric.co.jp

***Abstract*— The current resonant type DC-DC converter employs generally the pulse frequency modulation and its magnetizing inductance is set relatively low. For this reason, the magnetizing current through the converter causes a power loss under the light load condition. To solve this problem, a multi-oscillated current resonant type DC-DC converter has been proposed and then the advantage of its control method has been clarified, which can reduce power loss under light load condition and keep low switching noise. This paper deals with a novel reduction strategy of standby power consumption of the converter. As a result, the standby power consumption under no load condition is achieved below 60mW at 100V AC input and 150mW at 240V AC input, respectively. Furthermore, it is clarified that the slope of the resonant current envelope at soft start and end function in the standby mode influence the acoustic noise from the converter.**

Keywords; resonant converter, standby-power consumption, acoustic noise

I. INTRODUCTION

The current resonant type DC-DC converter, which has advantage of high efficiency, low noise and small size, is used widely in consumer electronics, telecommunication systems and so forth [1-12]. The pulse frequency modulation (PFM) is employed generally in this type of converter [1-12]. However, this type of converter has deteriorated problems, in which a magnetizing current through the converter causes a loss of power under the light load condition. Also, it is difficult to reduce power consumption under no load condition i.e. in the standby mode. So, it is necessary to use another isolated converter which is relatively large in order to reduce the standby mode power loss.

To solve these problems, a multi-oscillated current resonant DC-DC converter has been proposed [13-18]. It has been clarified in recent some papers that the high power efficiency (maximum one over 96% in DC-DC section) is achieved under the condition from the light load by using the PWM and self-oscillation [17, 18].

This type converter has adopted the intermittently switching mode in the standby mode [15]. In generally, the function of intermittently switching is able to reduce power consumption, but it has a problem with the acoustic noise compatibility.

This paper presents a novel standby control strategy for the multi-oscillated current resonant DC-DC converter, which is superior to the former paper. Furthermore, the reduction of the power consumption in the standby mode is discussed with considering the acoustic noise compatibility.

II. CIRCUIT CONFIGRATION

Figure 1 and 2 show the proposed multi-oscillated current resonant DC-DC converter and the timing chart, respectively. This converter consists of a half-bridge circuit, whose switches Q_1 and Q_2 which consist of MOSFET, are operated by a multi-oscillated current resonant driven by an IC with pulse-width modulation (PWM), and an auxiliary winding N_{P2} of the transformer, respectively.

In this converter, a multi-chip power module which consists of a control IC and two MOSFETs into one package is adopted. Furthermore, a startup circuit which is connected to the input voltage of this converter is included in the control IC of this module. Therefore, PWB pattern is minimized than they are composed as all discrete devices.

In the Fig. 1, an AC input is converted to DC voltage through the AC-DC rectifier bridge and PFC circuit which is normally used a PFC control IC in former step of this converter.

The leakage inductance of transformer is included in T_r (It is omitted in the figure). In the secondary side, a sub DC-DC converter is added for supplying the voltage to the system control (e.g. CPU and its peripheral). This sub DC-DC converter is also used in the standby mode. It is important to note that the isolation element is unnecessary such as AC-DC converter, in which its size is very small and the circuit configuration is very simple.

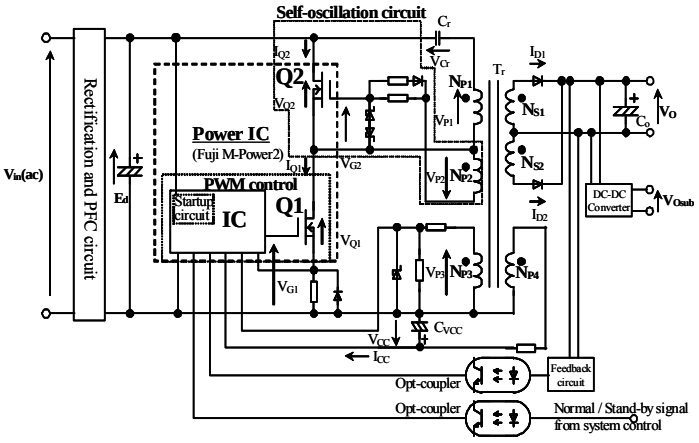

Fig. 1 Circuit configuration

By applying a gate voltage to Q_1 and Q_2 at turn-on and turn-off, switching power losses are reduced due to the zero-voltage switching (ZVS) and zero-current switching (ZCS).

In the isolated transformer T_r, the primary winding N_{P1} is loosely coupled to the secondary windings N_{S1} and N_{S2}, for in which the voltage of the leakage inductance is relatively large. Because of the resonant circuit with this leakage inductance and the resonant capacitor, the switching power losses of Q_1 and Q_2 are reduced.

A winding of transformer N_{P3} is added for timing detection of Q_1. The polarity of this winding is opposite to N_{P2}, which is used to drive Q_2. Moreover, the control IC turns Q_1 off before N_{P3} turns to negative. Therefore this converter prevents arm short automatically.

In this converter, to realize the novel standby operation, the winding N_{P4} for the power supply V_{CC} is coupled strongly to the secondary windings and it is electrically isolated from the secondary side. And the control IC detects the output voltage V_O indirectly by observing V_{CC} in the standby mode.

In the normal operation, the input voltage for this converter is regulated to 400 V DC by PFC circuit. On the other hand, in the standby mode, the input voltage for this converter is varied from about 140 to 340 V DC in universal input because a power supply to the PFC circuit is turned off for reducing power consumption.

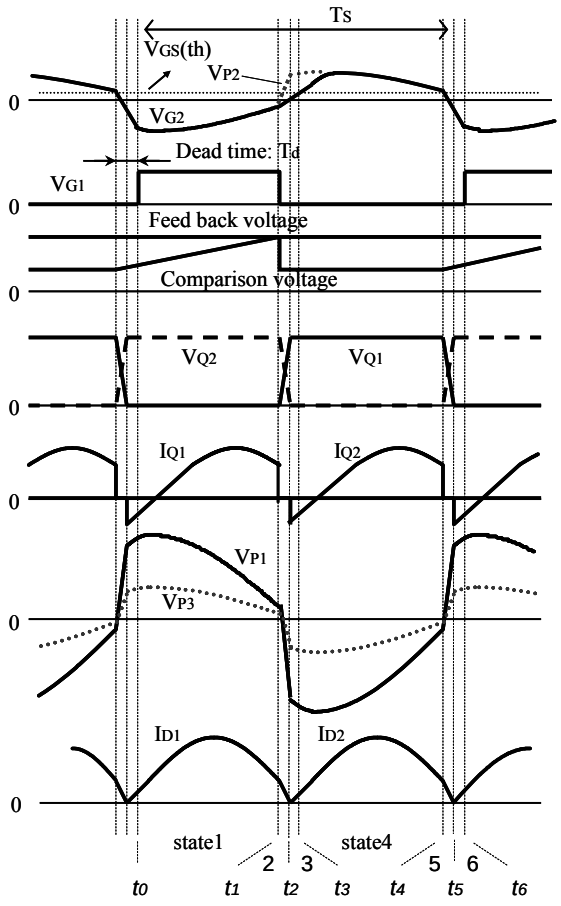

Fig. 2 Timing chart

III. Operation Principle

A. *Basically Operating mode (Normal Mode)*

Figure 3 shows the equivalent circuits of the converter shown in Fig. 1, which is divided into eight behavior states. Taking into account the combination of the eight states of behavior, they are further divided into four operating modes [16].

Figure 4 shows the simulated waveforms of the current and voltage for the four operating modes. From the results, the op-

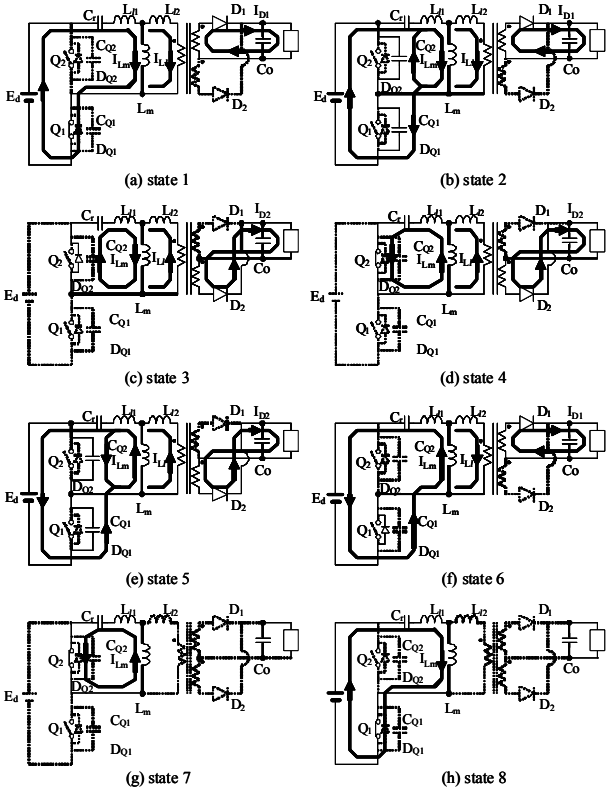

Fig. 3 Equivalent circuits and operation states

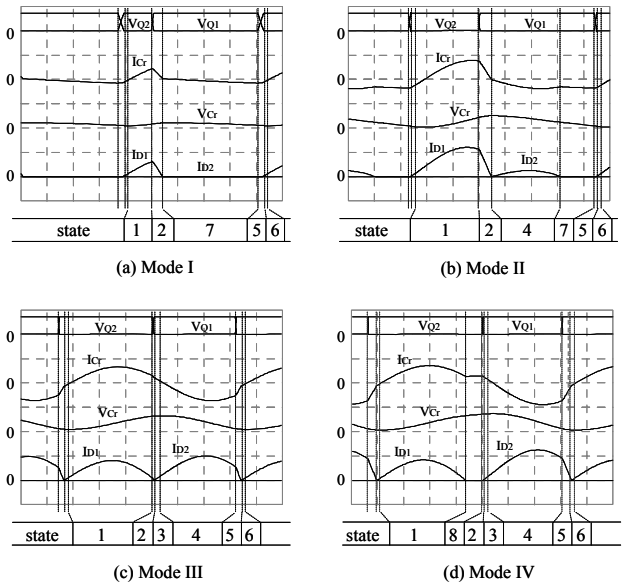

Fig. 4 Operation modes

erating modes appear in the order of I, II, III and IV when the load current is varied from the light load to the heavy load.

The operating modes I and II mainly appear at light load. The energy in C_r is discharged when the Q_1 turns off and Q_2 turns on, and charged by applying the output voltage E_d of the PFC when the Q_1 turns on and Q_2 turn off. Therefore, the energy is discharged to the secondary side through the transformer. However, because of the magnetizing inductance L_m is set relatively large when there is shortage of the energy discharged from C_r, operating state 7 appears, in which there is no discharging interval to the secondary side.

In the mode III, a ripple is reduced and smoothed by the leakage inductance L_{l2} of the secondary winding and the output capacitor C_o because the current flows continuously through D_1 and D_2, alternately.

The Mode IV appears when the duty ratio is almost over 50 %. In this mode, the state 8 appear where the power is not applied to the secondary side even when Q_1 turns on.

B. Standby Mode

Figure 5 shows block diagram of control circuit that is related to standby function and figure 6 shows the on period of Q_1 characteristic. In the standby mode, voltage V_{CS} of a capacitor C_{CS} determines the on period of Q_1.

Figure 7 shows the timing chart of standby mode. In the standby mode, the system control in the secondary side releases the pulled-up connection to the reference voltage of the control IC (approximately 5V). Then the control IC discharges C_{CS} with constant current I_{CS}, so the on-period of Q_1 is narrowed gradually as V_{CS} is decreasing, then stops switching in time (soft-end function).

When switching is stopped, supplying to the voltage of the control IC's power supply V_{CC} is also stopped, and then this voltage is reduced gradually by the power consumption of IC. And the output voltage V_O is also reduced by the power consumption of the secondary side, but the output voltage V_{Osub} for the system control of the secondary side is stabilized by the DC-DC converter in the secondary side.

If V_{CC} becomes under the threshold voltage of V_{BL}, the control IC starts charging C_{CS} by constant current I_{CS} and starts switching with the on period of Q_1 limited by V_{CS} (soft-start function).

As the switching is restarted, V_{CC} and V_O are increased. When V_{CC} reaches the threshold voltage of V_{BH}, the control IC changes to soft-end function.

That is, this converter operates in intermittently switching with soft-start and soft-end function. The on period of Q_1 and the peak of the resonant current increases and decrease gradually. And the slope of the resonant current envelope $\Delta I_{Crp}/\Delta t$ is able to be adjusted with C_{CS}.

Therefore, this function is expected to suppress acoustic noise because it is known that a drastic change of a current through the transformer causes an acoustic noise [15].

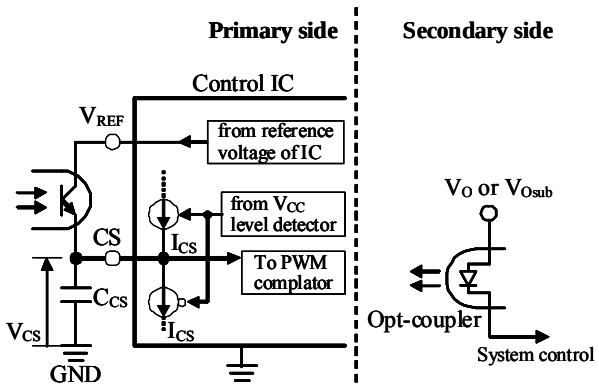

Fig. 5 Block diagram of control circuit (Related to standby function)

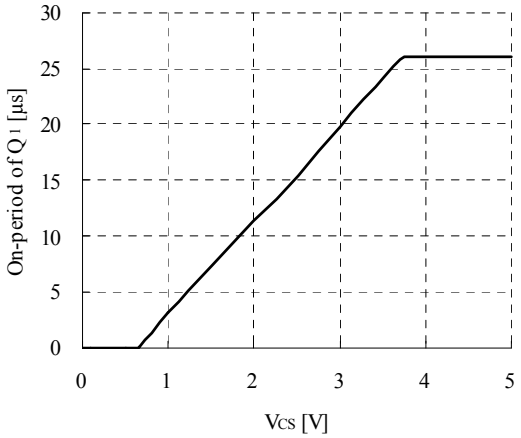

Fig. 6 On period of Q_1 characteristic

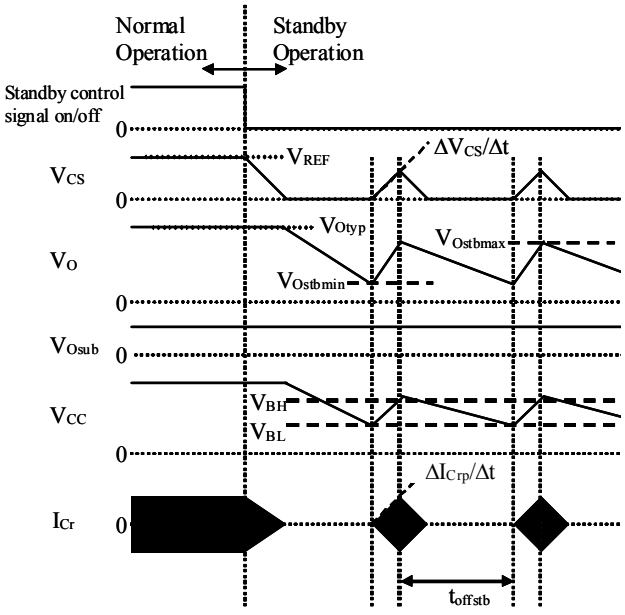

Fig. 7 Timing chart of standby mode.

In the standby mode, as mentioned, V_{CC} is regulated approximately between V_{BL} and V_{BH}. Because the coupling between the winding N_{S1}, N_{S2} and N_{P4} is strongly, the output voltage of V_O is proportional to the V_{CC}. So the output voltage V_{Ostb} in the standby state is given as:

$$V_{Ostb} = \left(\frac{T_{NS1}}{T_{NP4}}\right) \cdot V_{CC} \quad (1)$$

$$T_{NS1} = T_{NS2} \quad (2)$$

where, T_{NS1} , T_{NS2} and T_{NP4} are the winding number of N_{S1}, N_{S2} and N_{P4}.

To reduce standby power consumption in the secondary side, the maximum output voltage in the standby mode $V_{Ostbmax}$ must be lower than the output voltage rating V_{Otyp} in the normal operation, and given as:

$$V_{Ostb\max} \approx \left(\frac{T_{NS1}}{T_{NP4}}\right) \cdot V_{BH} \le V_{Otyp} \quad (3)$$

In addition, the minimum output voltage in the standby state $V_{Ostbmin}$ must be higher than the minimum allowable input voltage of the secondary DC-DC converter V_{Odcin} so as to supply voltage continually to the system control.

$$V_{Ostb\min} \ge V_{Odcin} \quad (4)$$

$V_{Ostbmin}$ is represented using P_{Sstb} which is power consumption in the secondary side in the standby mode.

$$V_{Ostb\min} = \sqrt{V_{O\max stb}{}^2 - \frac{2}{C_{CO}}\left(P_{Sstb} \cdot t_{offstb}\right)} \quad (5)$$

where, C_{CO} is the capacitance of the output capacitor, t_{offstb} is suspended period of intermittently switching in the standby mode and it is nearly equal with the fall time from V_{BH} to V_{BL} in V_{CC}. In this period, the control IC consumes almost constant current I_{CCstb} from the capacitor C_{VCC} which is connected with N_{P4} winding. Therefore, t_{offstb} is given as:

$$t_{offstb} \approx \frac{(V_{BH} - V_{BL})}{I_{CCstb}} \cdot C_{VCC} \quad (6)$$

where, C_{VCC} is the capacitance of V_{CC}.

IV. Standby Power Characteristics

A. *Standby power consumption characteristics*

Figure 8 shows experimental results of the power consumption characteristics. The experimental conditions are as follows: Input voltage $V_{in(ac)}$ = 100V-240V, Output voltage rating V_{Otyp}=24V, Output Rating $P_{o(typ.)}$ = 144W, Resonant Capacitor C_r=22nF, Resonant Inductance L_r= 320uH, Magnetizing Inductance L_m=1.8mH, Winding ratio of T_r T_{NP1}: T_{NS1} (=T_{NS2}): T_{NP2}: T_{NP3}:T_{NP4} = 59: 8: 5: 6: 6, Capacitance of the output C_{CO}=2200uF, Capacitance connected to V_{CC} winding C_{VCC} =470uF, Capacitance at CS terminal C_{CS} = 0.56uF – 2uF, Charge and discharge current from CS terminal I_{CS}=□±100uA

It is confirmed that the standby power consumption P_{in} under no load condition i.e. 0 mW of the output power P_O is below 60mW at 100V AC input and 150mW at 240V AC input, respectively. When the P_O is 50mW under the light load condition, P_{in} is below 150mW and 250mW at 100V and 240V AC input, respectively.

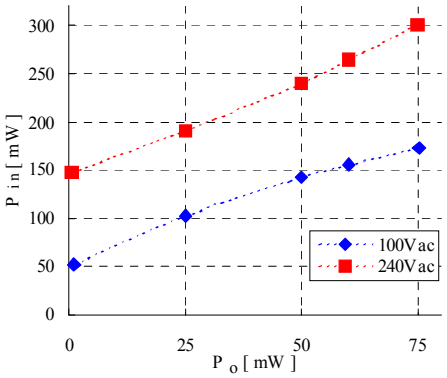

Fig. 8 Standby power consumption characteristics

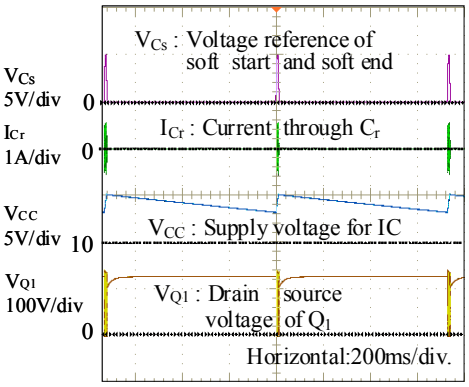

(a) Horizontal: 200ms/div. ($V_{in(ac)}$=100V)

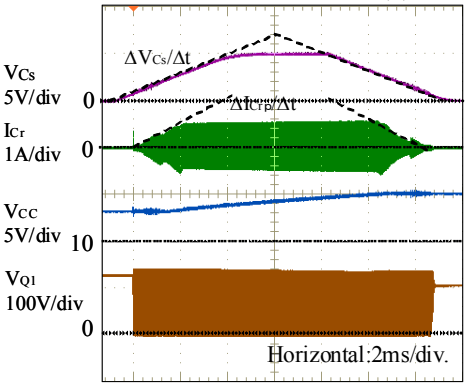

(b) Horizontal: 2ms/div. ($V_{in(ac)}$=100V)

Fig. 9 Switching waveforms in the standby mode. (a) 200ms/div. and (b)2ms/div. i.e.

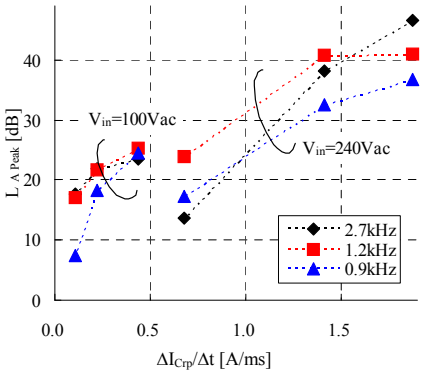

Fig. 10 A-weighted sound pressure characteristics in the standby mode

B. *Acoustic noise characteristics*

Figure 9 shows the switching waveforms in the standby mode. In Fig.9 (b), the horizontal axis is enlarged 100 times. It is seen in this figure that the peak of I_{Cr} is increased gradually as V_{Cs} is increased in the soft-start and soft-end function. And the slope of the resonant current envelope $\Delta I_{Crp}/\Delta t$ is determined by the slope of V_{Cs}.

Figure 10 shows experimental result of the sound pressure level characteristics, taking frequency of the acoustic noise f_A as a parameter. The measurement values are adopted the A-weighted sound pressure level considering the equal loudness contour. These frequencies f_A are selected from major 3 peaks of measured data. The measurement value of acoustic noise is represented as L_{Apeak}. In Fig.10, it is confirmed that the A-weighted sound pressure i.e. acoustic noise from this converter becomes large with increase in $\Delta I_{Crp} / \Delta t$. And the sound pressure level of the acoustic noise below 17dB at 100V AC input and 24dB at 240V AC input respectively is achieved.

V. CONCLUSION

Considering the acoustic noise compatibility, a novel reduction strategy of the standby power consumption is proposed and examined in the multi-oscillated current resonant DC-DC converter. As a result, this paper is conclude as follows,

(1) This converter is controlled by a combination of self-oscillation and a separated oscillation.

(2) This converter has eight states and four operating modes.

(3) In the novel standby control method, output voltage is controlled indirectly using the winding of the power supply for the control IC, which is coupled strongly to the secondary windings.

(4) In this converter, the standby power consumption below 60mW at 100V AC input and 150mW at 240VAC input at the no load respectively is achieved.

(5) The slope of the resonant current envelope $\Delta I_{Crp} / \Delta t$ at the soft start and soft end function affects the A-weighted sound pressure i.e. acoustic noise from the converter.

(6) The sound pressure level of the acoustic noise below 17dB at 100V AC input and 24dB at 240V AC input respectively is achieved.

Optimization and analysis of the characteristics of standby mode, and more detail analysis of acoustic noise will be reported in our next paper.

REFERENCES

[1] V. Volperian and S.Cuk, "A complete dc analysis of the series resonance converter, " in IEEE PESC 1982, pp85-100.

[2] R. L. Steigerwald, "High frequency resonant transistor dc-dc converters," IEEE Trans. Ind. Electron., vol. IE-31, pp.181-191, May 1984.

[3] R. L. Steigerwald, "Analysis of a resonant transistor dc-dc converter with capacitive output filter," IEEE Trans. Ind. Electron., vol. IE-32, pp.439-444, Nov. 1985.

[4] R. L. Steigerwald, "A comparison of half-bridge resonant converter topologies." IEEE Transactions on Power Electronics Vol. 3 No. 2, pp.174-182, April 1988.

[5] T. Duerbaum, "First harmonic approximation including design constants", INTELEC'98, pp.321-328, 1998.

[6] K. Morita "Novel Ultra Low-noise Soft Switching-mode Power Supply", INTELEC'98, pp.115-122, 1998.

[7] C. Chakraborty, M. Ishida, Y. Hori, "Novel half-bridge resonant converter topology realized by adjusting transformer parameters" IEEE Trans. on Industrial Electronics, vol. 49, no. 1, pp. 197-205, Feb. 2002.

[8] K. Kuwabara, H. Ota, "On the Output Increase of a Series Resonant DC-DC Converter", IEICE Technical Report, Vol.105, no.45, EE2005, pp.35-40, 2005.

[9] K.-H. Yi, G.-W. Moon, "Novel Two-Phase Interleaved LLC Series-Resonant Converter Using a Phase of the Resonant Capacitor," IEEE Trans. on Industrial Electronics, vol. 56, no. 5, pp. 1815-1819, May 2009.

[10] A. K. S. Bhat, "Analysis and Design of LCL-Type Series Resonant Converter" IEEE Trans. on Industrial Electronics, vol. 41, no. 1, pp. 118-124, Feb. 1994.

[11] K. Jin, X. Ruan, "Hybrid Full-Bridge Three-Level LLC Resonant Converter - A Novel DC-DC Converter Suitable for Fuel-Cell Power System," IEEE Trans. on Industrial Electronics, vol. 53, no. 5, pp. 1492-1503, Oct 2006.

[12] J.A. Sabate, M.M. Jovanovic, F.C. Lee, R.T. Gean, "Analysis and design-optimization of LCC resonant inverter for high-frequency AC distributed power system," IEEE Trans. on Industrial Electronics, vol. 42, no. 1, pp. 63-71, Feb 1995.

[13] M. Gekinozu, K. Kuroki, K. Mori, T. Fujita "Self-oscillated type current resonant DC/DC converter", IEICE Technical Report, EE99-58, pp.33-38. 2002.

[14] Y. Nishikawa, T. Nozawa, S. Igarashi, K. Kuwahara, N. terasawa "Multi-oscillated Current Resonant Converter", Annual Conference Record of EEEJ, Vol.4, pp.157-158, 2002.

[15] Y. Nishikawa, T. Nozawa, S. Igarashi, K. Kuwahara, N. Nozawa, H. Ota "A control method that reduce the conversion loss at a light load", Annual Conference of Japan, Industry Application Society, pp.631-632, 2002.

[16] R.Araki, O. Matsuo, H. Ota, M. Tuji, Y. Ishizuka, H. Matsuo "Static Analysis of Multi-Oscillated Current Resonant Type DC-DC Converter", IEICE Technical Report, EE2006-31, pp13-18, 2006.

[17] T. Sato, R. Araki, H. Ota, N. Higashi, Y. Ishizuka, H. Matsuo "Power Efficiency Analysis of a Multi-Oscillated Current Resonant Type DC-DC Converter", IEEE PESC'08, pp.1646-1650, 2008.

[18] T. Sato, H. Matsuo, H. Ota, Y. Ishizuka, N. Higashi, "Power Efficiency Improvement of a Multi-Oscillated Current Resonant Type DC-DC Converter Power Efficiency Analysis of a Multi-Oscillated Current Resonant Type DC-DC Converter", IEEE INTELEC'09, PC15-1, pp.1-5, 2009.